OTREC

FINAL REPORT

OREGON TRANSPORTATION RESEARCH AND EDUCATION CONSORTIUM

Performance Enhancement of Bridge Bracing Under Service and Extreme Loads

OTREC-RR-10-17
December 2010

A National University Transportation Center sponsored by the U.S. Department of Transportation's Research and Innovative Technology Administration

PERFORMANCE ENHANCEMENT OF BRIDGE BRACING UNDER SERVICE AND EXTREME LOADS

OTREC-RR-10-17

by

Peter Dusicka, PhD, PE
Assistant Professor
email: dusicka@pdx.edu
phone: (503) 725-9558
Portland State University

Max Stephens, Research Assistant
and
Kate Fox-Lent, Research Assistant

for

Oregon Transportation Research
and Education Consortium (OTREC)
P.O. Box 751
Portland, OR 97207

OTREC
OREGON TRANSPORTATION RESEARCH AND EDUCATION CONSORTIUM

December 2010

Technical Report Documentation Page

1. Report No. OTREC-RR-10-17	2. Government Accession No.	3. Recipient's Catalog No.
4. Title and Subtitle Performance Enhancement of Bridge Bracing Under Service and Extreme Loads		5. Report Date December 2010 6. Performing Organization Code
7. Author(s) Peter Dusicka, Assistant Professor Max Stephens, Research Assistant Kate Lent-Fox, Research Assistant		8. Performing Organization Report No.
9. Performing Organization Name and Address Portland State University Department of Civil and Environmental Engineering PO Box 751 Portland, OR 97207		10. Work Unit No. (TRAIS) 11. Contract or Grant No.
12. Sponsoring Agency Name and Address Oregon Transportation Research and Education Consortium (OTREC) P.O. Box 751 Portland, Oregon 97207		13. Type of Report and Period Covered 14. Sponsoring Agency Code
15. Supplementary Notes		

16. Abstract

The purpose of this study was to develop and demonstrate the concept of retrofitting bridge brace elements with fiber reinforced composites in order to provide restraint against buckling. The advanced materials consisted of a combination of fiber reinforced polymer (FRP) composite pultruded sections and wet lay-up wraps, intended to be applied in the field. A selected number of prototype retrofit bracing specimens were constructed and tested using reverse cyclic loading, and the performance of these specimens was characterized by their compressive strength and their overall hysteretic behavior.

The results of this exploratory study have shown that slender bracing members retrofitted with FRP sections show an improved level of performance. All retrofitted specimens showed an improved compressive strength in the linear elastic and plastic deformation range of the slender bracing member. The cyclic behavior exhibited only a marginal improvement, however, due to failure modes at the bolted connections of the brace. Further modification of the brace had marginally improved the cyclic performance. Despite the challenges associated with the connection failures of the retrofitted members, the demonstration has shown that the developed concept of applying fiber reinforced composites has a potential to effectively restrain slender bracing members from buckling and improve the compressive resistance. Further testing needs to be conducted to evaluate a more optimal implementation for resisting cyclic loads.

17. Key Words bridge, steel bracing, retrofit, fiber reinforced polymer (FRP)	18. Distribution Statement No restrictions. Copies available from OTREC: www.otrec.us

19. Security Classification (of this report) Unclassified	20. Security Classification (of this page) Unclassified	21. No. of Pages 28	22. Price

ACKNOWLEDGEMENTS

This project was funded by the Oregon Transportation Research and Education Consortium (OTREC) and Portland State University. Their support is gratefully acknowledged.

DISCLAIMER

TABLE OF CONTENTS

LIST OF TABLES

LIST OF FIGURES

EXECUTIVE SUMMARY

The demand on aging bridges continues to increase under service loads resulting from progressively larger truck loads, and under extreme loads resulting from engineers' improved understanding of the seismic risk. Truss bridges, steel girder diaphragms and braced substructures are comprised of slender steel structural elements that are crucial in resisting various loads and are typically designed primarily for tension. Their susceptibility to buckle under compressive loads results in compressive resistance that is well below the yield strength capacity, a contribution often discounted in design. Also, buckling induced asymmetric and pinched hysteretic behavior of these elements typically results in degrading hysteretic energy dissipation under seismic loading and can lead to premature failure caused by localized plastic strains. A retrofit measure was experimentally investigated in order to increase load capacity by enhancing the compressive resistance under monotonic loading and to improve the seismic response under cyclic loads.

A buckling restrained brace (BRB) was recently developed for buildings as a structural member that is capable of attaining compression strength governed by material yielding rather than global buckling. This is achieved by encasing a ductile core in a steel tube filled with mortar. The steel tube and mortar act to restrain the encased member from buckling, thereby increasing its compressive strength. Furthermore, BRBs have the advantage of exhibiting ductile behavior in cyclic tension and compression, making them well suited for resisting earthquake loads. BRBs have been primarily used for new building construction and are not always suitable for bridge retrofits due to their heavy weight, specialized connection requirements and the need for complete member replacement. However, the concept of externally restraining buckling along the length of the member can have a direct impact as an effective retrofit measure for bridges with slender steel elements. Accordingly, this report develops and demonstrates the concept of retrofitting bridge brace elements with fiber reinforced polymer (FRP) materials in order to provide restraint against buckling. A selected number of prototype retrofit bracing specimens were constructed and tested using reverse cyclic loading. The performance of these specimens was characterized by their compressive strength and their overall hysteretic behavior.

The results of this exploratory study have shown that slender bracing members retrofitted with FRP sections show an improved level of performance. All retrofitted specimens showed an improved compressive strength in the linear elastic and plastic deformation range of the slender bracing member. The cyclic behavior exhibited only a marginal improvement, however, due to failure modes at the bolted connections of the brace. Further modification of the brace marginally improved the cyclic performance. Despite the challenges associated with the connection failures of the retrofitted members, the demonstration has shown that the developed concept of applying fiber reinforced composites has a potential to effectively restrain slender bracing members from buckling and improve compressive resistance. Further testing needs to be conducted to evaluate a more optimal implementation for resisting cyclic loads.

1.0 INTRODUCTION

1.1 BACKGROUND

The demand on aging bridges continues to increase under service loads resulting from progressively larger truck loads, and under extreme loads such as earthquakes resulting from engineers' improved understanding of the risk. Since bridges form an integral part of the transportation infrastructure, their integrity is crucial to maintaining the proper function and efficiency of the transportation network. Steel girder bridge diaphragms, truss spans and braced substructures are often comprised of slender structural elements that are crucial in resisting various loads and are typically designed primarily for tension. Their susceptibility to buckle under compressive loads results in compressive resistance that is well below the yield strength capacity. The compression contribution is often discounted in design, but if utilized to its full potential can present additional load-carrying capacity for the structure. Under seismic loading, which is characterized by large reversed deformation cycles, asymmetric and pinched hysteretic behavior of buckled elements results in degrading hysteretic energy dissipation. More importantly, localized plastic strain caused by the bending and straightening can lead to failure under a low number of reversals (*Park et al 1996*).

Means of retrofitting these types of structural components for earthquakes is limited to primarily field welding strengthening methods (*FHWA 2006*). Enhancing the compression capacity by delaying or minimizing buckling would lead to improved performance under these extreme loading conditions. With many lift span and truss bridges in the Portland area, the benefit would be realized regionally. It also would have an impact nationally as steel bridges with bracing elements were a common means to span longer distances and many are nearing the end of their design life. A new method is needed that takes advantage of modern materials.

A buckling restrained bracing (BRB) was recently developed for new building construction as a structural member that is capable of attaining compression strength that is governed by material yielding rather than global buckling. This is achieved by encasing a ductile core with a steel tube filled with mortar, which restrains the steel core from buckling (*Black et al 2004, Lai & Tsai 2004*). Special interface material between the steel core and the mortar allows for plastic strains in the core without composite action, thereby limiting the strength to a desired and predetermined value. BRBs have the advantage of exhibiting ductile hysteretic behavior in tension and compression, making them well suited for resisting cyclic loads. They have been exclusively applied to new building construction in order to achieve higher-than-standard levels of seismic performance. The American Institute of Steel Construction recently added design provisions for BRBs in their seismic specifications for buildings (*AISC 2005*), and the industry has started to adopt them in design.

1.2 LITERATURE REVIEW

In the last few decades, buckling-resistant braced frames have become increasingly popular in Asia and the western United States as many experimental and analytical studies have

demonstrated the effectiveness of BRBs in improving the hysteretic behavior of slender bracing members. Experimental studies conducted by Rezai et al. (2000), Nakamura et al. (2000), Iwata et al. (2000), Lai and Tsai (2001), Black et al. (2004), and Xie (2004) investigated the overall cyclic behavior of BRBs and the effects of various bracing properties on this behavior. In addition to displaying the improved compressive behavior of restrained bracing members, it was commonly found that bracing properties such as the type of de-bonding material, section shape, connection type, and the brace restraint type influence the hysteretic behavior of the braces. Black et al. (2004) and Dicleli and Calik (2008) additionally utilized experimental data to develop analytical models to simulate the hysteretic behavior of restrained braces under cyclic loading. Work by Rezai et al. (2000) and Iwata et al. (2000) expanded the experimental scope of restrained bracing by examining the use of commercially available BRBs as hysteretic fuse elements in concentrically steel-braced frames. Both experiments demonstrated the potential for restrained bracing to be used as hysteretic dampers in steel structures, whereby the bracing generally demonstrated a stable hysteretic response under cyclic loading. Work by Ko and Field (2003) summarizes the development of the unbounded brace, and works by Ko and Field (2003), Xie (2004), and Lai and Tsai (2004) discuss the current uses of restrained bracing in new construction and seismic retrofits.

1.3 FIBER REINFORCED POLYMER

While buckling restrained bracing has demonstrated much experimental success and has been implemented in primarily new construction of large buildings, utilizing BRBs for the widespread retrofit of infrastructure such as bridges presents other different challenges. As current BRBs are commonly fabricated using traditional materials such as steel tubing and mortar, retrofit applications are restricted by structure redundancy and weight limitations. It is thus not viable to utilize current BRB technology on such preexisting structures as bridges where it is less feasible to remove and replace a large number of members, and undesirable to add significant weight, surface area or significantly alter the load path. As bridges are of immense public importance, there is an interest in developing a method with which to retrofit existing bracing members with light-weight buckling restraints. Accordingly, this report presents study results associated with the use of light-weight fiber reinforced polymer (FRP) sections to restrain single-angle bracing members from buckling.

FRP composites are starting to become a viable material for use in our infrastructure, primarily for the purpose of retrofitting concrete bridge components and also as prefabricated bridge decks. However, research into FRP composites combined with steel has been extremely limited and even more so in applications of expected plastic behavior. One of the benefits of using FRP for retrofit of concrete components is the ability to apply the material in the field to any shape surface using a wet lay-up process. Such methods are often used to provide confinement for seismic retrofits of columns or as wrap for deteriorated concrete beams. On the other hand, FRP bridge decks are prefabricated from pultruded sections, typically in the form of tubes that provide high strength and stiffness. These can be used as deck replacements to reduce dead load on bridges; such was the case locally on the Broadway Bridge in Portland (Dusicka et al 2004). The benefits of the in-field application of FRP and the stiffness characteristics of pultruded sections are combined with in-situ steel elements to provide a retrofit-based buckling restraint as conceptualized in Figure 1.1a. Such an application would result in minimal added weight for gravity loads and surface area for wind loads. Since the pultruded section mainly provides

restraint and does not necessarily directly participate in the load resistance, the system load path would not be significantly affected other than the benefit realized from the enhanced compression capacity of the retrofitted member.

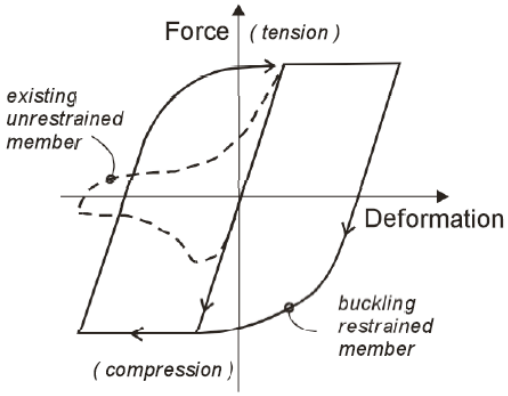

(a) Anticipated Axial Cyclic Response

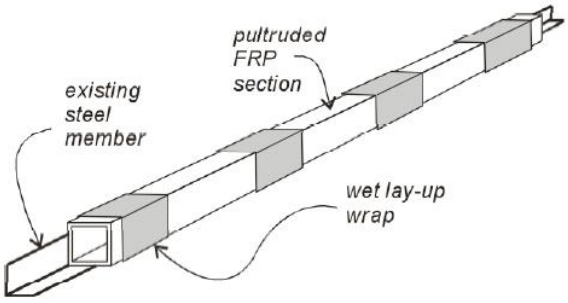

(b) Example of Field Installed Retrofit Measure.

Figure 1.1: Concept Illustration of Performance Enhancement Using FRP Materials

The purpose of this study was to develop and demonstrate the concept of a bridge-brace retrofit measure with fiber reinforced composites that provide restraint against global compression buckling. Following a survey of relevant bridges in the state of Oregon, it was determined that slender single-angle members are commonly used as bracing elements, as shown by the example in Figure 1.2. Thus for the purpose of the experiments, the cyclic behavior of single-angle members retrofitted using pultruded FRP sections was investigated. All tests were conducted in accordance with provisions provided by the 2005 American Institute for Steel Construction (AISC) Seismic Handbook.

Figure 1.2: Example of Bridge Bracing Using Mild Steel Angles

2.0 TEST SETUP

2.1 TEST MATRIX

Primary testing focused on 2-inch x 2-inch x 1/4-inch angle members retrofitted using pultruded FRP sections of varying shapes (specimen specifications to be discussed in Section 2.2). Two tests were conducted on plain angles to obtain benchmark data. At least two specimens were prepared using each FRP shape, one with a partial fiber wrap and one with a full fiber wrap. Each member was subjected to a loading program which consisted of increasing displacements during elastic and post-yield cycles. This protocol follows the loading sequence given in the AISC Seismic Handbook, and is discussed in Section 2.4.

2.2 TEST SPECIMEN

Figure 1.1b depicts the general form of the test specimens used in the study. The specimens consisted of A36 steel grade 2-inch x 2-inch x 1/4-inchcore angle members and a pultruded FRP restraining member attached using glass fiber wrap applied around the assembly.

2.2.1 Steel Angle Members

All angle members were from the same mill batch, and had a reported yield strength of 45.9 ksi and a reported ultimate strength of 70.5 ksi. The 2-inch x 2-inch x1/4-inch angles were chosen as the core steel sections because they are compact according to AISC table B4.1, which limits local buckling of the section. These members were cut to a length of 85 inches to accommodate the dimensions of the test apparatus (specifications to be discussed in Section 3). The critical buckling load of each specimen was calculated using the equation 2-1 below:

$$P_{cr} = \frac{\pi^2 EI}{(kL)^2} \quad \textbf{(2-1)}$$

Where P_{cr} is the critical buckling strength, E is the modulus of elasticity, I is the moment of inertia of the cross sectional area, k is the effective length factor, and L is the length of the member. Using the material properties of steel, the geometric properties of the angle sections, and the constraint properties of the test apparatus, the critical buckling strength was determined to be 22.3 kips. This value will be compared to the buckling strength of the benchmark specimens.

In preparing the core angle members for buckling restraint application, the sharp corner of each member was smoothed using a grinder to effectively increase the outer radius of curvature, and the mill scale on the legs was left unchanged. Each connection consisted of four staggered 13/16-inch holes for use with A325 ¾-inch bolts, and all connections were reinforced using 1.5-inch x ¾-inch flat bar to account for the reduced section of the bolted connection. Two 6-inch lengths of 1.5-inch x ¼-inch flat bar were welded perpendicular to the face of one leg of each angle, and two 6-inch lengths of ¼-inch threaded rod was welded to the flat bar for use in instrumentation. Two TML type YFLA-5 post-yield strain gauges were additionally applied to the outside leg of each core section at approximately $L_{eff}/2$ and $L_{eff}/3$. A total of nine members were prepared in total. Two prepared core members were set aside for use as a control group while all others were reinforced using restraining members and an epoxy fiber wrap.

2.2.2 Buckling Restraint FRP Sections

The pultruded FRP restraining members used in this experiment consisted of series 525 structural shapes manufactured by Strongwell. The shapes used consisted of round tubes with 3-inch diameters and square-cross-section tubes of 4x4x1/4 inches, 2x2x1/4 inches, and 3x3x1/4 inches. These cross sections are shown in Figure 2.1 and correspond to (a), (b), (c), and (d), respectively.

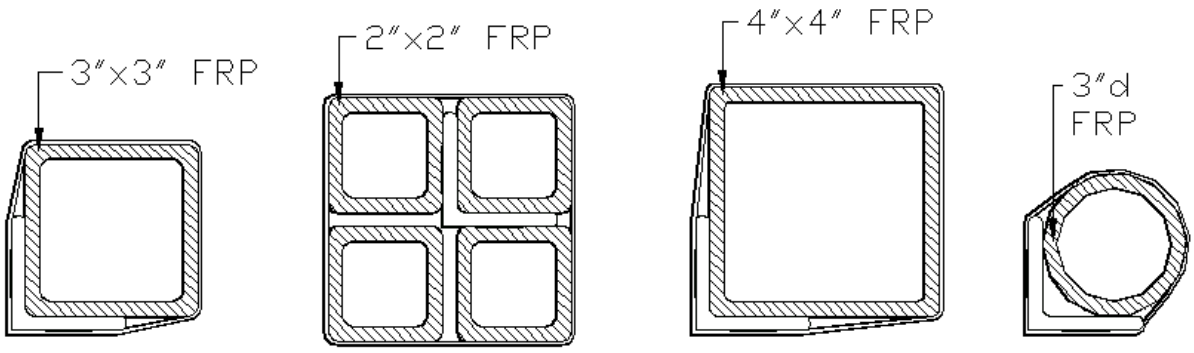

Figure 2.1: Cross Section of All Specimens Retrofitted with FRP.

The mechanical properties of the fiberglass used in these pultruded shapes have been provided by the manufacturer. These values were determined from coupon tests, and are displayed in Table 2.1. All given values are ultimate properties in the "lengthwise" direction of the structural shapes.

Table 2.1: Mechanical properties of the fiberglass used in the pultruded FRP shapes.

MECANICAL PROPERTY	
Tensile Strength LW	30 ksi
Tensile Strength CW	7 ksi
Flexural Strength LW	30 ksi
Flexural Strength CW	10 ksi
Elastic Modulus LW	2500 ksi
Elastic Modulus CW	NA

LW = Lengthwise
CW = Crosswise

Two specimens were created using each FRP shape. All restraining sections were cut to lengths of 60 inches, and were roughened with sand paper in order to promote the bonding of the fiber wrap. Prior to fixing the prepared restraining sections to the angle members, a de-bonding layer was placed on the angles in order to reduce friction between the restraining member and the angle. The de-bonding agent consisted of cellophane wrap.

2.2.3 Application of FRP Sections

The final step in preparing the test specimens was to permanently secure the restraining sections to the angle members. This was accomplished by applying a wet lay-up of epoxy and a fiber reinforced composite (FRC) to the angle-restraining tube assembly. The lay-up materials consisted of a 20-foot x 54-inch roll of Tyfo SEH-51 fiber wrap with a strongly unidirectional weave, and a Tyfo S two part epoxy. To begin the lay-up process the epoxy components were mixed to the manufacturer's specification, and were hand worked into precut sections of fiber weave. The precut sections were measured to provide two uniform layers of fiber wrap to each specimen. The weave was applied to the angle-restraining tube assembly so that the strong fiber direction was perpendicular to the length of the angle. As the provided fiber material was not wide enough to cover the full width of the restraining section, two separate fiber sheets of 54

inches and 6 inches were applied to each fully wrapped specimen. Cellophane wrap was used to tightly secure the wrap to the bracing member. This wrap was kept on each specimen throughout the curing and testing process. For the purpose of the partially wrapped specimens, fiber wrap was only applied in 12-inch lengths at the center and each end of the restraining member. All specimens were given a cure time of at least seven days, and 500-watt lights were used to expedite the curing process. For separate material property tests, two pieces of 12 inches x 12 inches were also saturated, pressed and layered on top of each other, with the strong-direction fibers aligned. These were left to cure on a section of polyvinyl sheeting and were later cut to standard coupon dimensions for tensile testing according to ASTM D 3039. The direction of the fibers was identified and five strips of fiber wrap, 15 millimeters wide, were cut with their long dimension parallel to the strong direction of the fibers. The strips were then trimmed to 25 centimeters in length and the ends saved for use as grips during testing. A dozen additional strips of 2-inch x13-inch fiber wrap were saturated and applied perpendicularly to the outside face of a section of FRP and on one leg of a piece of angle from the same 2x2x1/4. Two strips were applied to each section so that each contacted the steel over a 2-inch x 2-inch area, two strips so that each contacted the steel over a 2-inch x 4-inch area, and two strips so that they contacted the steel over a 2-inch x 6-inch angle. The same dimensions were used for the fiber wrap applied to the FRP section. All specimens were saved to test the shear strength of the surface bond between the fiber wrap and the core angle section.

2.2.4 Modified Specimens

In order to alleviate connection failures, modifications to the specimens were made along the length of three of the specimens. This modification consisted of drilling holes through the cured fiber wrap and core steel section with the intention of reducing the cross section to weaken the member. The modified specimens included two of the angle members retrofitted with the 3-inch x 3-inch FRP tube, and one member retrofitted with the 3-inch-diameter FRP tube. One of the members retrofitted with the 3-inch x 3-inch square FRP tube was modified by drilling 5/8-inch-diameter holes at 3 inches center to center, while the other was modified by drilling ¾-inch holes at 2 inches center to center. The specimen retrofitted with the 3-inch-diameter FRP tube was modified by drilling ¾-inch holes at 2 inches center to center. Figure 2.2 shows the modified section of one of the members retrofitted with the 3-inch x 3-inch FRP tube after testing.

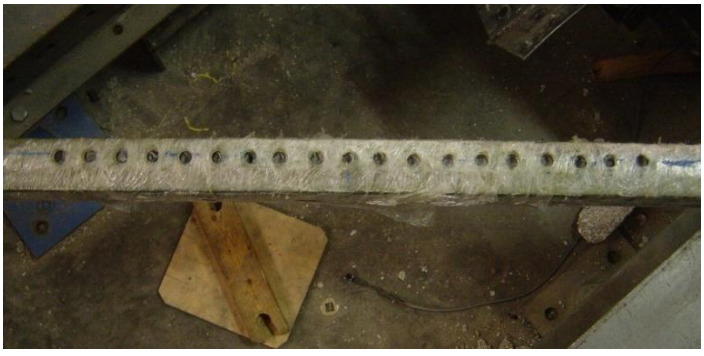

Figure 2.2: Modified Section of a Specimen Retrofitted with a 3-inch x 3-inch FRP Tube.

2.3 Test Apparatus

Figure 2.3 shows the horizontal load frame constructed in order to test the angle specimens. The beams of the load frame comprised W10x26 with two rows of ¾-inch holes, at a vertical and horizontal spacing of 4 inches on center, drilled through the web along the entire length. One 19-foot length was available and one 15-foot length was spliced to a 4-foot length. The two beams were positioned parallel, 43 ¾ inches apart, and fixed in place by reaction plates bolted between the beams. The entire assemblage was bolted to pedestals to raise it 12 ¾ inches above the laboratory floor. A 100 kip hydraulic actuator was secured to one reaction plate such that the centerline of the actuator aligned with the center of the reaction plate. The load cell for the horizontal actuator was calibrated using an Omega LC 101 30 kip load cell. The calibration was determined in terms of voltage output up to 20 kips and was assumed to be linear up to the full 100 kip capacity of the load cell.

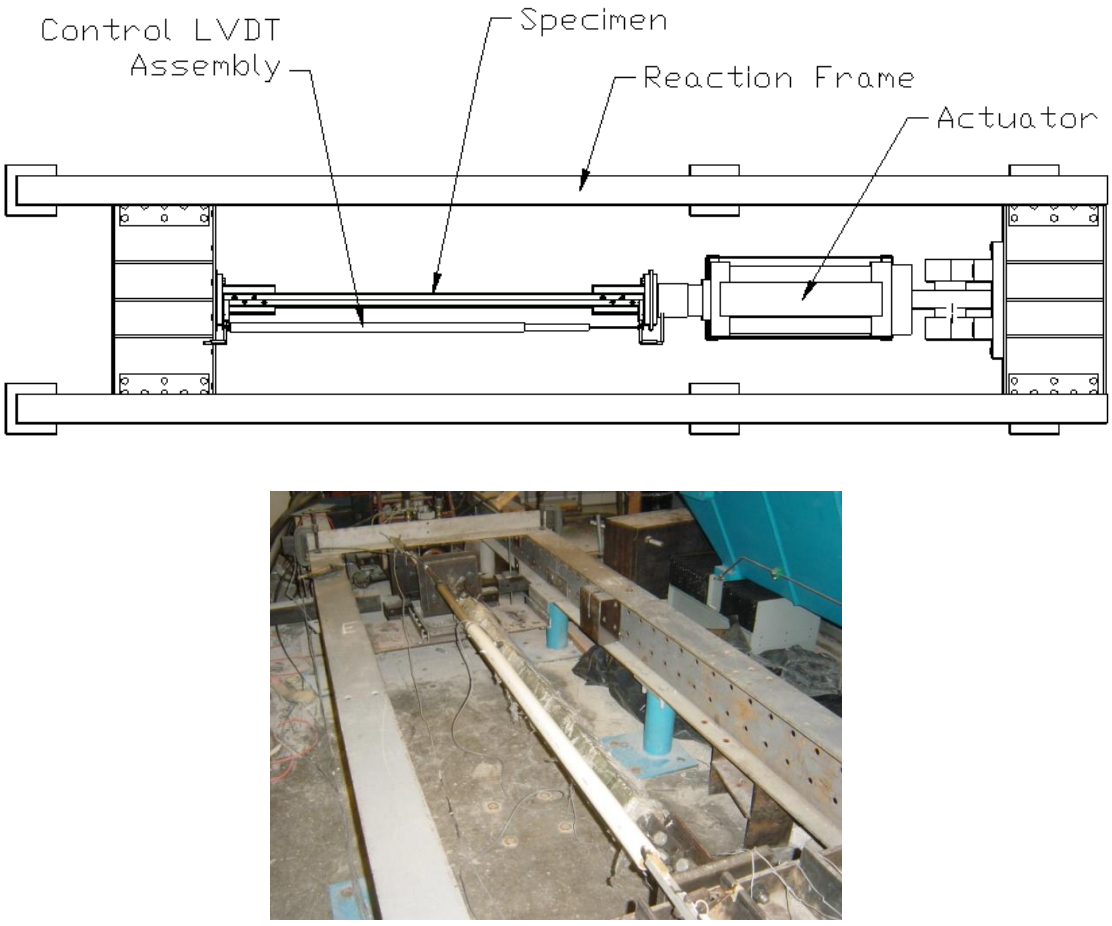

Figure 2.3: Test Apparatus

2.4 Instrumentation

In addition to the two post-yield strain gauges placed on the core steel sections, four strain gauges were placed on the outside of the fiber wrap. Three gauges, placed 2 inches, 7 inches and 30 inches from the end of the restraining tube, were oriented in order to measure strain along the strong direction of the wrap. One gauge, placed 30 inches from the end of the wrap, was oriented in order to measure strain along the weak direction of the wrap. Control displacement was measured using a 20-inch Novotechnik Linear Variable Displacement Transducer (LVDT) fixed to the core section of each specimen (LVDT 1). The transducer was placed into a 1.75-inch-diameter PVC pipe with a universal joint fixed to one end, and the assembly was suspended from the specimen via the threaded rods discussed in section 2.2.1. Two 2-inch Novotechnik LVDTs were additionally placed between each fixed connection and the specimen in order to monitor slip in the bolted connection (LVDTs 2 and 3). Figure 2.4 shows the basic instrumentation plan. A LabView VI was constructed to record data during the experiment. All data was recorded using a National Instruments data acquisition device (DAQ).

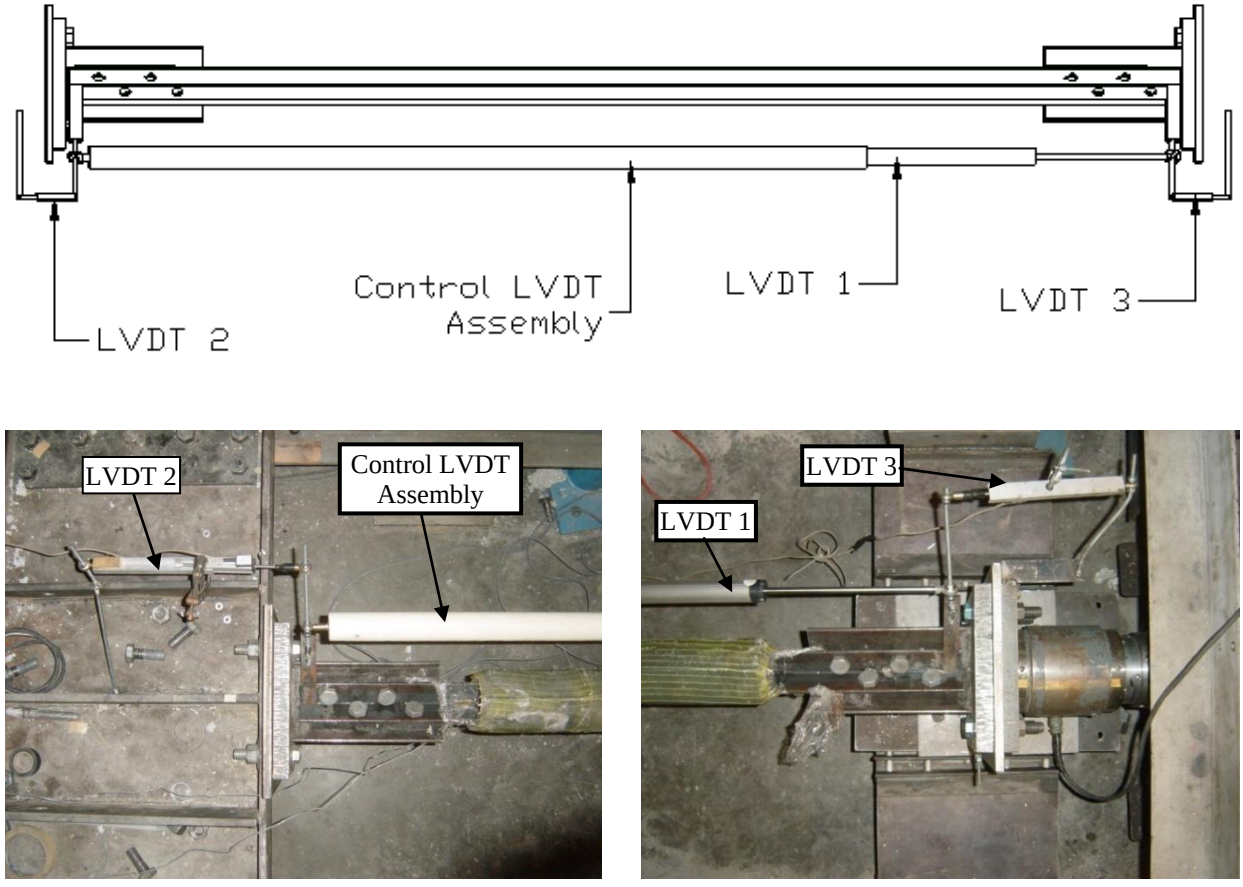

Figure 2.4: Instrumentation Layout.

2.5 LOADING PROTOCOL

The loading protocol used in this experiment follows the specifications provided in the AISC seismic provisions. Each test was conducted by controlling the level of axial deformation, Δ_b, imposed on each specimen, and each specimen was subjected to cyclic loading at increasing displacement values. All displacement values were measured in relation to the deformation at yield and the deformation at a 1% design story drift of a single-level frame. The yield deformation value, Δ_{by}, was calculated using the relationship between strain and the length of the angle. This relationship is given by equation 2-2:

$$\delta = \frac{F_y}{E} L \qquad \textbf{(2-2)}$$

where δ is the deformation, F_y the yield stress, E the modulus of elasticity and L the length of the member. Taking F_y to be 36 ksi, E to be 29,000 ksi, and L to be 80 inches, Δ_{by} was calculated to be 0.1 inch. The deformation at the design story drift of 1%, Δ_{bm}, was calculated by examining the deformation of a 45-degree bracing member in a single-level frame (see Figure 2.5). Assuming the length of the bracing member is 80 inches, this deformation was determined to be 0.4 inch. The control displacement values used in each test ranged from $0.25\Delta_{by}$ to $1.0\ \Delta_{by}$ in the elastic range and $1.0\Delta_{bm}$ to $6.0\Delta_{bm}$ in the plastic range of the core steel member. Two cycles were conducted at each deformation, and each test was run until the specimen failed or the limits of the actuator were reached.

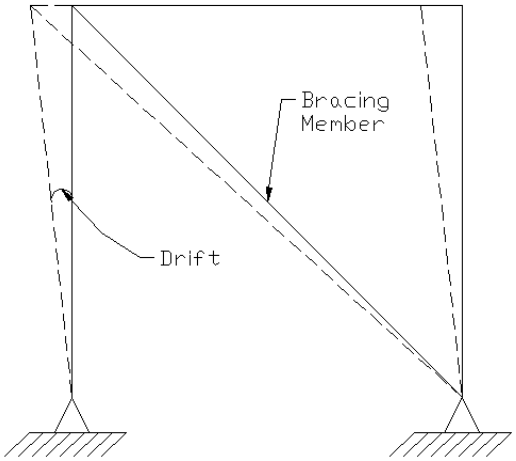

Figure 2.5: Single-Story Frame Used to Calculate the Deformation of the Bracing Member at Design Story Drift.

3.0 SUMMARY OF RESULTS

3.1 TEST OBSERVATIONS

The shape of the pultruded FRP section used to retrofit each member had a significant impact on the behavior of the specimen during testing. The modified and unmodified specimens retrofitted using the 3-inch-diameter FRP tube experienced a large amount of global flexure during the plastic deformations of the core section (see Figure 3.1b). The compressive strength of these specimens was increased despite the bending; however, this behavior brings into question the adequacy of the 3-inch-diameter FRP section to effectively restrain slender bracing members. The unmodified specimens retrofitted with the square 2-inch x 2-inch, 3-inch x 3-inch, and 4-inch x 4-inch FRP tubes did not experience bending on a global level. However, they experienced bending between the FRP tube and the bolted connection during the plastic deformations of the core section (see Figures 3.1c and 3.1d). This bending resulted in a complete loss of compressive strength and, in some cases, the separation of the FRP section from the core angle and block shear at the bolted connection. The modified specimens retrofitted with the square 3-inch x 3-inch FRP tube did not experience bending at the bolted connection, and did not experience large amounts of global bending in the early plastic deformations of the core angle member. As the flexural integrity of the FRP tubes on all the specimens retrofitted with square FRP appeared to remain intact throughout testing, it seems these sections are stiff enough to effectively restrain slender bracing members from buckling.

Partially and fully wrapped specimens did not behave differently during testing. The partially and fully wrapped specimens retrofitted with the 3-inch-diameter FRP tube both experienced large global bending in the plastic deformations of the core angle section. The partially and fully wrapped specimens retrofitted with the 2-inch x 2-inch and 4-inch x 4-inch FRP tubes all experienced bending between the end of the FRP tube and the bolted connection. The limits of the fiber wrap were not reached during any of the tests due to the weak flexural strength of the 3-inch-diameter FRP section, and the bending experienced between the FRP tube and the bolted connection of all specimens retrofitted with the square FRP sections.

The behavior of the retrofitted specimens with modified sections helped to give insight as to the deformation of the core angle member relative to the fiber wrap and FRP tube. At the beginning of the tests, the holes through the fiber wrap and the core angle section of all the modified specimens lined up. As the specimens experienced deformation, the holes began to move relative to one another. This behavior shows that the core angle sections moved independently of the fiber wrap. As the FRP tubes are theoretically bonded to the fiber wrap, but not the core section, the movement of the core section relative to the fiber wrap suggests that the core angles moved independently of the FRP tubes. If this is the case, the pultruded FRP sections do not directly participate in load resistance, and the load path of the retrofitted members is not significantly affected.

3.2 FAILURE MODES

Table 3.1 shows a summary of the test results for all specimens tested, including failure mode, drift at failure, and ultimate loads in tension and compression. It should be noted that the results from the specimens retrofitted with 2-inch x 2-inch FRP tube have not been presented due to early connection failures in the tests. As was expected, both benchmark angles lost compressive strength and failed in compression due to global buckling. Figure 3.1a shows a benchmark specimen which has experienced global buckling. The specimens retrofitted using the 3-inch-diameter FRP tube displayed an increased compressive strength until the FRP tube failed in flexure. Once this occurred, the core angle member buckled, and the hysteretic behavior of the specimens returned to that of unrestrained sections. This behavior can be seen in Figure 3.3 below. Figure 3.1b shows the flexural failure of the FRP on a specimen retrofitted with the 3-inch-diameter FRP tube. The specimens retrofitted using the 4-inch x 4-inch square FRP tube also displayed improved compressive strength in the linear elastic range of the core angle member. However, both specimens experienced local buckling between the bolted connection and the FRP tube.

This local buckling resulted in a loss of all compressive strength provided by the restrained portion of the specimen, and the hysteretic behavior returned to that of an unrestrained member. The FRP section additionally separated from the core angle member as a result of the local buckling. This can be seen in Figure 3.1c. The specimens retrofitted with the 3-inch x 3-inch FRP tube also displayed an improved compressive strength in the linear elastic and plastic drift ranges of the core angle member. The unmodified section, and the section modified with 5/8-inch holes drilled 3 inches center to center both lost compressive strength due to local buckling between the bolted connection and the FRP tube, while the section modified with ¾-inch holes drilled 2 inches center to center experienced a tensile failure of the core angle section early in the plastic drift range. Following local buckling, the hysteretic behavior of the unmodified section and the section modified with 5/8-inch holes drilled 3 inches returned to that of unrestrained sections, as all compressive strength provided by the restrained section was lost. Local buckling between the connection and FRP tube can be seen in Figure 3.1d

Table 3.1: Summary of the failure mode of all test specimens.

FRP TUBE GEOMETRY	CORRESPONDING HYSTERETIC PLOT	DRIFT AT FAILURE	MAX TENSION (KIP)	MAX COMPRESSION (KIP)	FAILURE MECHANISM
Benchmark	Figure 3.2 (a)	$4.5\Delta_{bm}$	57.1	20.4	Global Buckling
Benchmark	Figure 3.2 (b)	$6.0\Delta_{bm}$	54.3	22.5	Actuator Stroke Out/Global Buckling
3" Diameter Circle*	Figure 3.3 (a)	$3.0\Delta_{bm}$	42.6	32.7	Flexure Failure of FRP/Tensile Failure in Core Section
3" Diameter Circle	Figure 3.3 (b)	$4.0\Delta_{bm}$	54.7	44.1	Flexure Failure of FRP
4"x4" Square	Figure 3.4 (a)	$1.0\Delta_{bm}$	63.4	45.5	Local Buckling/Block Shear at Connection
4"x4" Square	Figure 3.4 (b)	$3.5\Delta_{bm}$	55.2	50.4	Local Buckling/Block Shear at Connection
3"x3" Square	Figure 3.5	$5.0\Delta_{bm}$	55.4	48.4	Local Buckling at Connection/Block Shear at

					Connection
3"x3" Square*	Figure 3.4 (a)	$2.5\Delta_{bm}$	50.4	46.9	Local Buckling at Connection/Tensile Failure in Modified Section
3"x3" Square*	Figure 3.4 (b)	$2.0\Delta_{bm}$	44	46.5	Tensile Failure in Modified Section

*Modified specimens. See section 2.2.4.

.

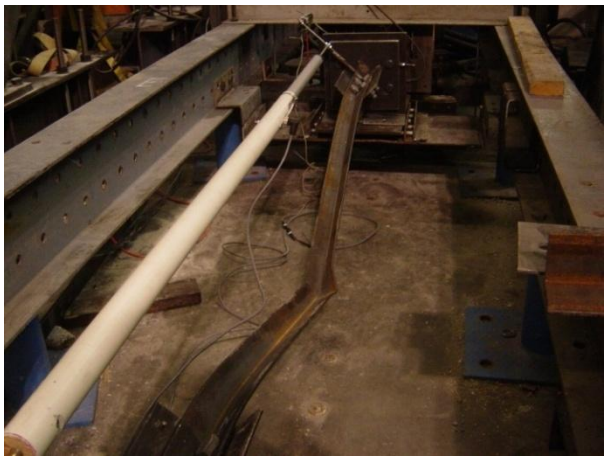

(a)

(b)

(c)

(d)

Figure 3.1: The flexural buckling of a benchmark specimen. (b) The flexural buckling of a specimen retrofitted with a 3-inch-diameter FRP tube. (c) Local buckling between the bolted connection and a 4-inch x 4-inch FRP tube. (d) Local buckling between the bolted connection and a 3-inch x 3-inch FRP tube.

3.3 CYCLIC BEHAVIOR

Force deformation hysteresis plots were developed for each specimen using deformation data collected from LVDT 1. These plots are displayed in figures 3.2 through 3.6. Figure 3.2 shows the force deformation plots of the benchmark specimens. These hysteresis plots show an unsymmetrical force deformation relationship in tension and compression due to the flexural buckling of the specimens in compression. While these specimens reached yield stresses in tension, they only reached stresses comparable to those estimated using Euler's buckling relationship in compression. Figure 3.3 shows the force deformation plots for the specimens retrofitted using the 3-inch-diameter FRP tube. These plots show that the specimens had improved compressive strengths in the linear elastic and smaller plastic drift ranges of the core steel section. Figure 3.4 displays the force deformation hysteretic behavior of the specimens

retrofitted using the 4-inch x 4-inch square FRP tubes. These specimens also demonstrated a large improvement in compressive strength in the linear elastic displacement range of the core section. Figure 3.5 shows the force deformation hysteresis plots of the modified specimens retrofitted using the 3-inch x 3-inch FRP tubes. These specimens not only displayed a large compressive strength improvement in the linear elastic and early plastic deformations of the core steel member, but also an improved overall hysteretic behavior. Figure 3.6 shows the force deformation hysteresis plot of the unmodified specimen retrofitted using the 3-inch x 3-inch FRP tube. This specimen demonstrated a large improvement in compressive strength in the linear elastic displacement range of the core section.

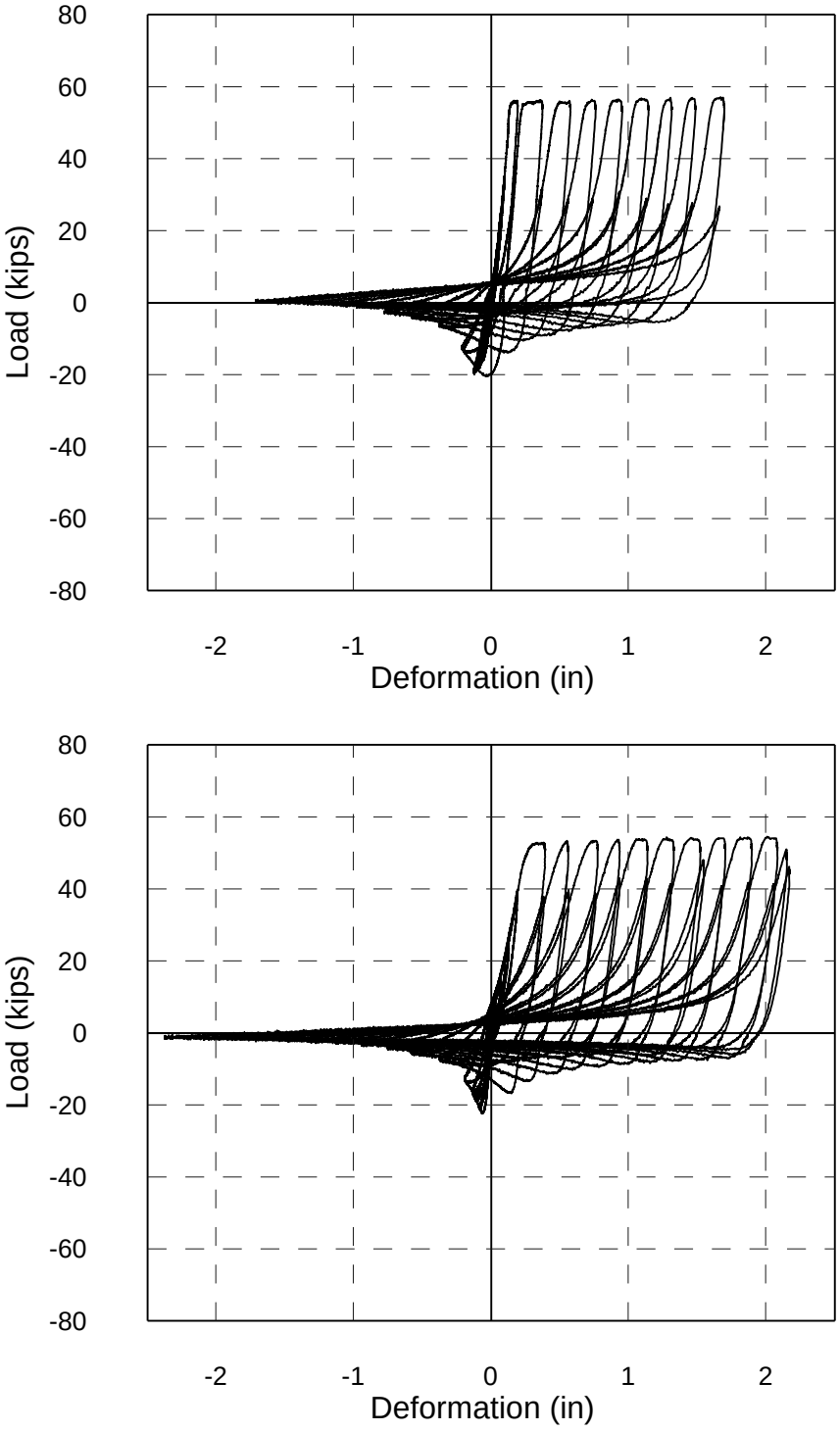

Figure 3.2: Force Deformation Hysteresis Plots of the Benchmark Specimens.

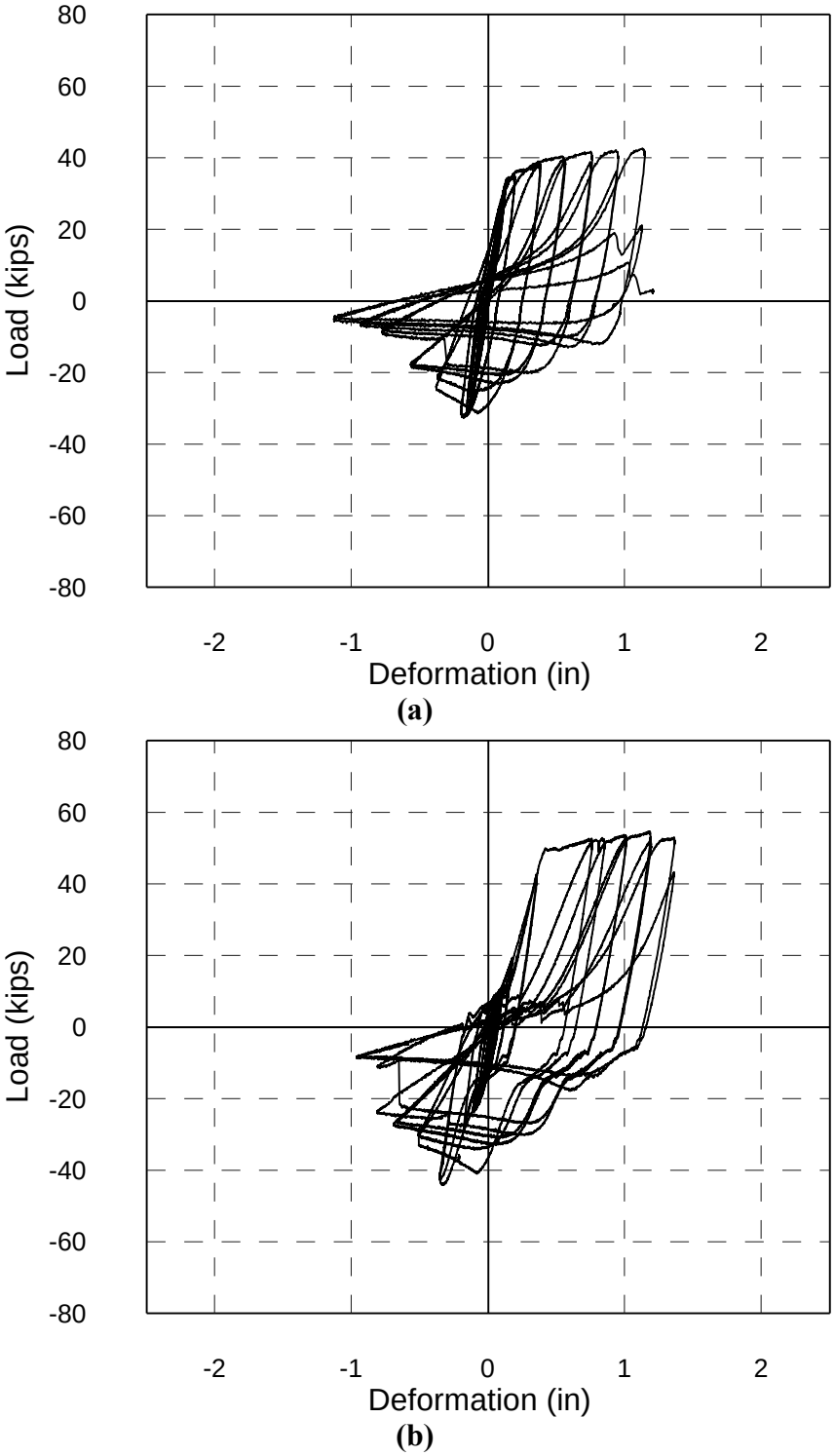

Figure 3.3: Force deformation hysteresis plots for specimens retrofitted with a 3-inch-diameter FRP tube (a) fully wrapped and (b) partially wrapped. (a) had a modified section with ¾-inch holes at 2 inches center to center.

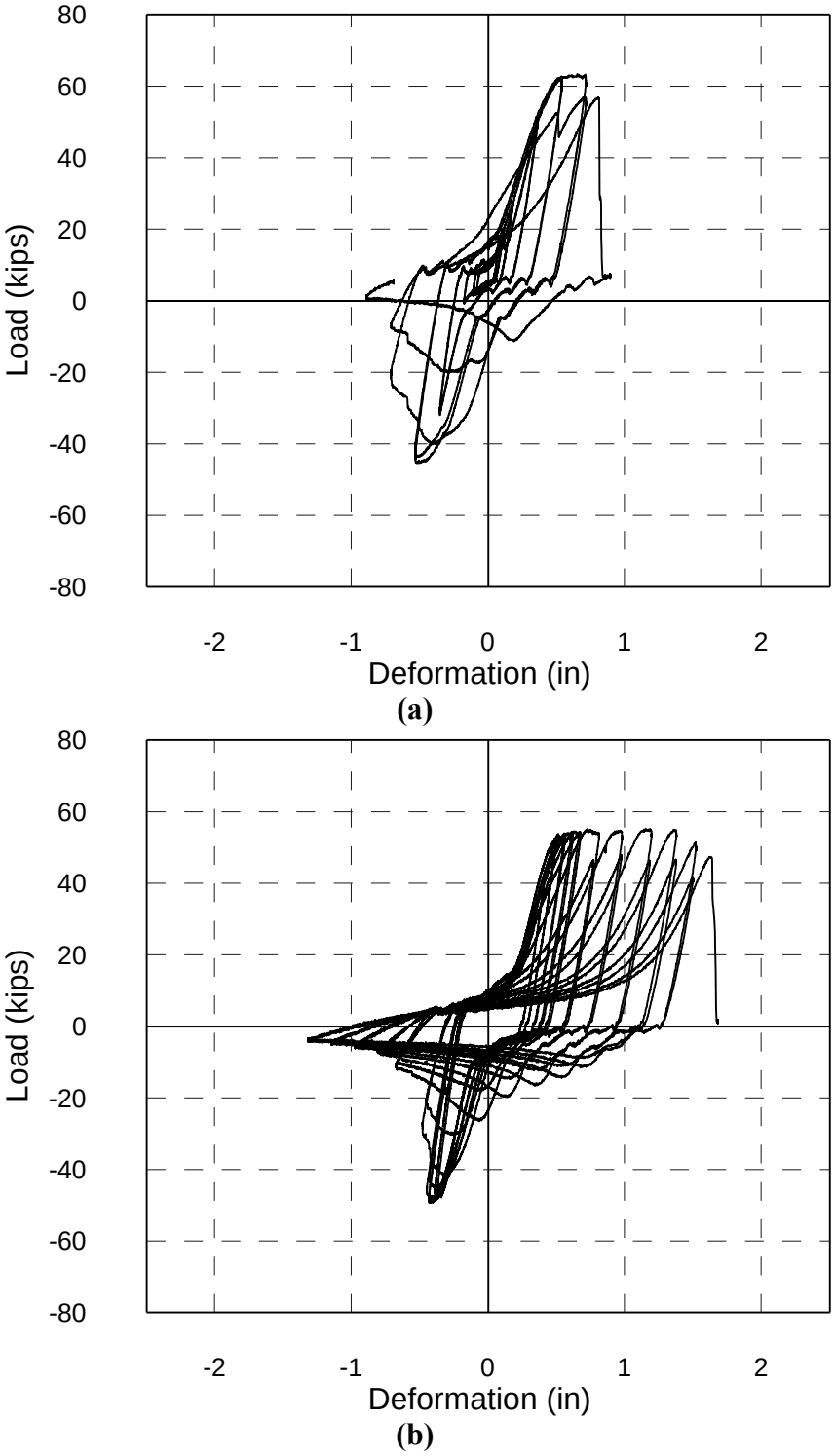

Figure 3.4: Force deformation hysteresis plots for specimens retrofitted with 4-inch x 4-inch square FRP tube (a) fully wrapped and (b) partially wrapped.

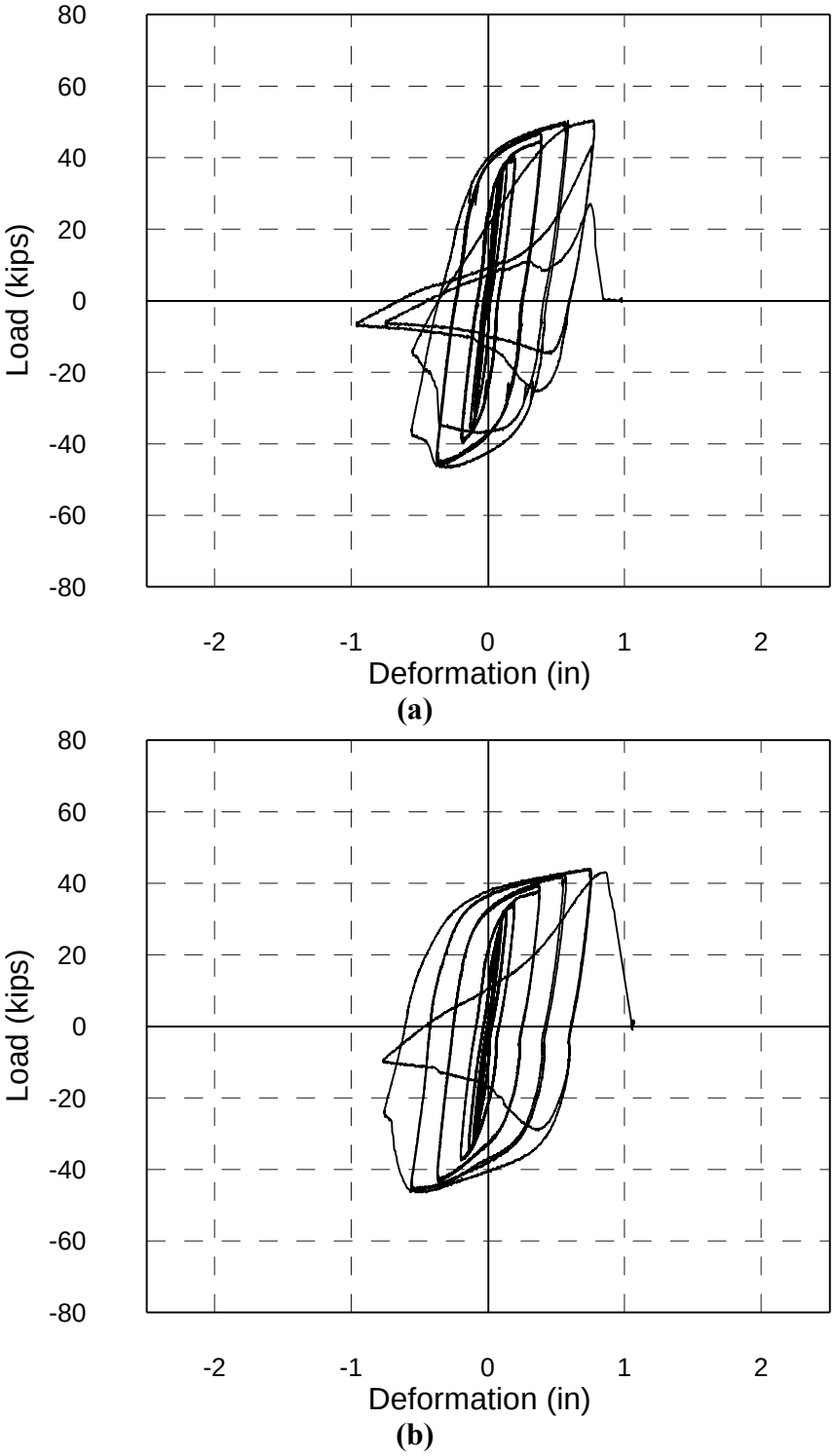

Figure 3.5: Force deformation hysteresis plots for specimens retrofitted with the 3-inch x 3-inch FRP tube with modified sections. (a) has been modified with 5/8-inch diameter holes at 3 inches center to center and (b) has been modified with ¾-inch holes at 2 inches center to center.

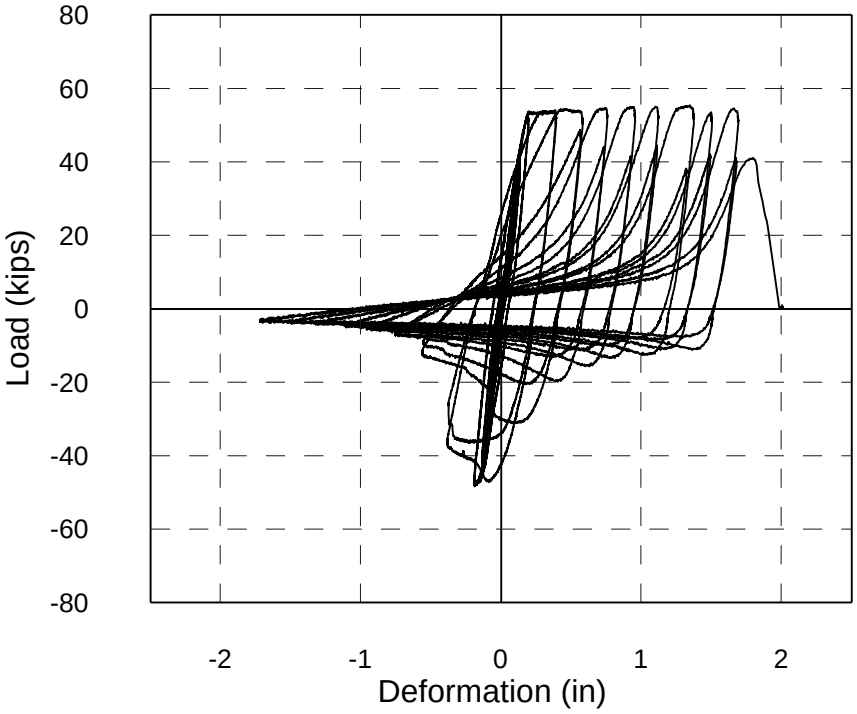

Figure 3.6: Force deformation hysteresis plot for the specimen retrofitted with the 3-inch x 3-inch FRP tube with an unmodified section.

4.0 FUTURE TESTING

While members retrofitted using FRP showed an improvement in compressive strength during the elastic drift cycles, the hysteretic behavior of the members remained largely unchanged due to local buckling between the bolted connection and FRP tube. The hysteretic behavior of the specimens with modified core angle sections to limit the effects of local buckling at the connections showed a slight improvement in the elastic and early inelastic drift cycles. However, the core angle section of these members generally experienced a tensile failure prior to the flexural failure of the FRP tube.

Due to the challenges regarding local buckling between the bolted connection and the FRP tube, it is thus suggested that future testing be conducted using double angle members as the core steel sections. Using these members, reinforcing can easily be added to prevent local buckling at the bolted connection. Figure 4.1 shows the cross section of potential retrofit specimens created using double angles.

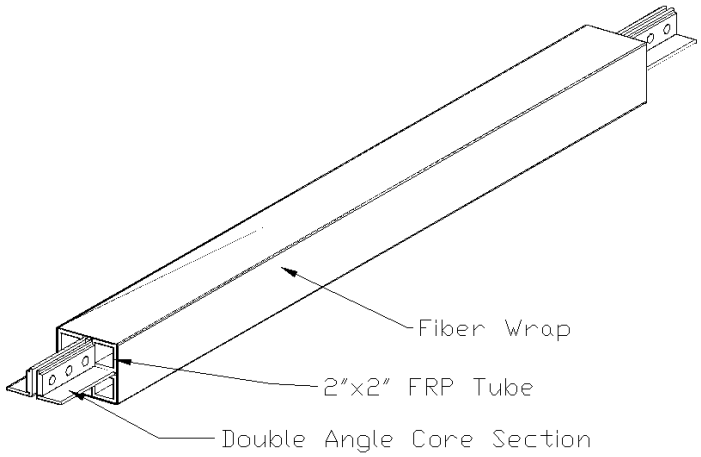

Figure 4.1: Future Test Specimens Created Using Double Angles.

Using the same overall test setup and loading protocol described for the single-angle specimens, testing was conducted on a double-angle benchmark specimen and double-angle retrofit member consistent with the section shown in Figure 4.1. The benchmark specimen displayed a force-deformation hysteresis plot similar to those shown by the single-angle benchmark specimens. The retrofit member displayed an increased compressive strength than that of the benchmark specimen; however, it failed due to block shear at the connection. It appears this failure was due to an inadequate application of the reinforcement plates at the bolted connection, and could easily be avoided in the future. The specimen did not show signs of local buckling.

5.0 SUMMARY AND CONCLUSION

This report presented a concept and experimental results from an exploratory research project investigating the use of FRP to restrain steel angle bracing members from buckling. Specimens retrofitted using FRP displayed an increased compressive strength in the elastic deformation range of the core angle section. However, the hysteretic behavior of the members remained largely unchanged due to local buckling between the bolted connection and the start of the FRP tube. The specimens that displayed an improved hysteretic behavior were those which were weakened within the core section in order to lower the demand on the entire brace. While this approach was successful in the early plastic deformation range of the core angle member, such a large amount of the cross section was removed from the core angles in these specimens that both specimens experienced tensile failure.

Despite the fact the hysteretic behavior of the retrofitted members remained largely unchanged due to failures at the bolted connection, extruded FRP sections have displayed the ability to adequately restrain and increase the compressive strength of single-angle bracing members. All of the retrofitted members displayed a compressive strength greater than the control case of a bare angle, which corresponded closely with the theoretical critical buckling equation. Thus, the compressive performance of the bracing members was enhanced by the FRP sections, even though the cyclic behavior remained unchanged in larger deformations. Additionally, the bolted connection of the test specimens could be modified to prevent local buckling between the FRP tube and the bolts, which would improve the overall hysteretic behavior of the bracing members. It is difficult to justify such an action, however, as the connection detail used in testing is consistent with bracing connections used in practice.

6.0 REFERENCES

AISC (2005), Seismic Provisions for Structural Steel Buildings, American Institute of Steel Construction, Chicago, IL.

Adluuri, S., & Madugula, M. K. (1996). Flexural Buckling of Steel Angles. Journal of Structural Engineering.

Black C.J., Makris, N. and Aiken, I.D. (2004), "Component Testing, Seismic Evaluation and Characterization of Buckling-Restrained Braces", Journal of Structural Engineering, ASCE, Vol. 130, No. 6.

Dicleli, M., & Calik, E. E. (2008). "Physical Theory Hysteretic Model for Steel Braces." Journal of Structural Engineering , 1215-1228.

Dusicka, P., Aldana, T. and Mueller, W.H. (2005) "Evaluation and Field Application of FRP Deck Panels for Drawbridge Deck Replacement", Proceedings of Advanced Materials for Construction of Bridges, Buildings and Other Structures IV, Maui, HI.

FHWA (2006), Seismic Retrofitting Manual for Highway Structures: Part 1 – Bridges, Federal Highway Administration.

Iwata, M., Kato, T., & Wada, A. (2000). "Behaviour of Steel Structures in Seismic Areas." Rotterdam: Balkema.

Ko, E., & Field, C. "The Unbonded Brace: From Research to Californian Practice."

Lai, J.W. and Tsai K.C. (2004), "Research and Application of Double-Core Buckling Restrained Braces in Taiwan", Proceedings of the 13th World Conference on Earthquake Engineering, Vancouver, Canada.

Mohan, S., Rao, N., & Lakshamanan, N. (2005). Flecural and Local Buckling Interaction of Steel Angles. International Journal of Structural Stability and Dynamics, 43-162.

NBI (2005), National Bridge Inventory, Federal Highway Administration, Washington, DC.

NHRTP (2002), Highway Research and Technology: The Need for Greater Investment, Report of the National Highway R&T Partnership.

OTREC (2006), University Transportation Center Strategic Plan, Oregon Transportation Research and Education Consortium, Portland, OR.

Nakamura, H., Maeda, Y., Sasaki, T., Wada, A., Takeuchi, T., Nakata, Y., et al. (2000). "Fatigue Properties of Practical-Scale Unbonded Braces." Nippon Steel Corporation.

Park Y.S., Iwai, S., Kameda H., Nonaka, T. (1996), “Very Low Cycle Failure Process of Steel Angle Members”, Journal of Structural Engineering, ASCE, Vol. 122, No. 2.

Rezai, M., Prion, H., Tremblay, R., & Bouatay, N. (2000). “Seismic Performance of Brace Fuse Elements for concentrically Steel Braced Frames.” Rotterdam: Balkema.

USDOT (2006), “Research, Development and Technology Plan – 6th Edition”, US Department of Transportation, Washington, D.C.

Xie, Q. (2004). State of the art buckling-restrained braces in Asia. Journal of Construtional Steel Research , 727-748.

P.O. Box 751
Portland, OR 97207

OTREC is dedicated to stimulating and conducting collaborative multi-disciplinary research on multi-modal surface transportation issues, educating a diverse array of current practitioners and future leaders in the transportation field, and encouraging implementation of relevant research results.